23rd ABCM International Congress of Mechanical Engineering
December 6-11, 2015, Rio de Janeiro, RJ, Brazil

EXPERIMENTAL DETERMINATION OF THE S-N DIAGRAMS OF BUTT WELDED JOINTS OF AUSTENITIC AISI 316 L STAINLESS STEEL

Fábio Brongar Milech
Kleber Eduardo Bianchi
Universidade Federal do Rio Grande - FURG
Av. Itália, km 8,
Bairro Carreiros
Rio Grande – Brazil

Abstract. *Nowadays the use of stainless steels as the base metal of mechanical structures is increasing, because of the availability in the market of easy-to-find alloys, which combine good weldability, mechanical strength and oxidation resistance. The critical spots of these structures usually are the joints and the main failure mechanism is fatigue. In the case of welded joints, the methodology of assessment is a matter of great concern to the designer, because these joints are sites of defects and high residual stresses, emerged from the welding process itself. The present study aimed to obtain the S-N fatigue curves of a butt welded joint under transversal loading, adopting specimens made of AISI 316L austenitic stainless steel, which were divided in three different groups: a) specimens with raw weld beads - no machining of bead reinforcement; b) specimens with machined weld beads in order to remove the face and root reinforcements, and c) specimens for base metal evaluation (no weld). Subsequently, the results were compared with data taken from Eurocode and American Welding Society Standards: Eurocode 3 - part 1.9 (2003) and AWS D1.1 (2010), as well as the Recommendations of IIW (International Institute of Welding) (HOBBACHER, 2008). In this context, plates of AISI 316 L stainless steel with a thickness of 6 mm were robot welded in a single pass, with bead transversal to rolling direction, and subsequently machined to give the final shape to the specimens. Metallographic and tensile tests were conducted to evaluate the weld joint quality. No significant defects were found and the mechanical strength of welded specimens was superior to that of base metal specimens. After that, the specimens were tested using cyclic loads in a servo hydraulic machine, in order to obtain the S-N diagrams. For the three tested groups of specimens, the fatigue life exceeded the values suggested by the cited standard guidelines and recommendations in cases of medium or low stress range values. However, when the specimens were subjected to high stress range values, the performance to fatigue failure was below of the expected result. The very good response under medium and low stress ranges was more expressive in the group of specimens with machined reinforcements, which presented much higher fatigue life than the no machined specimens. Thus, it was observed that the application of a relatively simple post-welding technique - the removal of the face and root reinforcements - resulted in an important increase in the specimens fatigue life. Finally, all the results obtained suggest that the guidelines and recommendations for welded joints design should consider the stainless steels as a group apart from the general structural steels.*

Keywords: *Welded joints, Fatigue, SN diagram, Stainless steel AISI 316 L.*

1. INTRODUCTION

The methodology of assessment for determining adequate dimensions, materials and manufacturing parameters of a welded part must take into consideration the particularities of this kind of mechanical component. First of all, the most important life criterion to be considered is fatigue failure. A second important aspect is related to the presence of flaws and tensile residual stresses in the weld bead vicinity, caused by the welding process. The magnitude of the stress concentration factor associated with the weld bead geometry, the presence of small cracks, as well as the magnitude of tensile residual stresses (oftentimes near the yield strength of the parent metal), are predominant aspects in relation to the nominal stress. Additionally, the presence of flaws in the weld bead region usually causes the absence of a crack initiation period (Branco, *et al.*, 1999; Zhang and Maddox, 2009; Lassen and Recho, 2012).

To encompass these aspects, standard codes directed to steel structures assessment usually provide information and procedures based on data obtained in extensive tests programs, performed over specimens that were welded in field conditions. So, the natural variability of materials and manufacturing processes in the field is replied in the specimens, which means that both components – real part and specimen – present the same magnitude of residual stresses and flaws. This is the approach, for example, of Eurocode 3 – Section 1.9 – Fatigue (2003), AWS D1.1 (2010), as well as the Recommendations of International Institute of Welding (Hobbacher, 2008) and CIDECT (*Comité International pour le Développement et l'Etude de la Construction Tubulaire*) (Wardenier, *et al.*, 1995; Zhao, *et al.*, 2000).

These cited procedures adopt some general considerations, in order to promote a simplified and robust process of welded joints assessment. First of all, the list of covered materials comprises only ordinary structural steels and aluminum. Additionally, the mechanical part or structure should be composed of bars, sheets or plates, arranged in well-known configurations, just as girders or trusses, or even simple reinforced beams, columns or gantries. Another important consideration is that the joints, welded or screwed, are the critical sites where cracks propagate. So the dimensions of the linking elements shall be prescribed in order to guarantee a proper fatigue life of the joints (and not the contrary). Finally, there are three procedures for specifying welded joints: *i)* classification method, *ii)* tension of hot-spot method and *iii)* fracture mechanics method. The first of these methods is widely used in preliminary design phases.

The classification method adopts two sets of S-N diagrams separately, for normal and shear stresses in the bead, which are used by the designer along the dimensioning process. The methodology is simple and robust, because is based in a very simple thought: a higher S-N curve represents a better fatigue performance of the joint. So, if the designer is in a preliminary step of the project, he or she is able to adopt a more appropriate joint configuration. For example, one could adopt cast steel nodes, which promote transversal butt joints at the extremities of the tubes of a truss, instead of a fillet welded K or X joint configuration. Such a design decision could provide a better fatigue performance and an easy to make structure (Haldimann-Sturm and Nussbaumer, 2008; Nussbaumer, *et al.*, 2010).

Another interesting issue is that different sets of joint configuration and direction of load in the weld bead could present a similar fatigue performance. In simple words, distinct welded joints could share the same S-N diagram.

A S-N curve can be described by three simple parameters: *i)* fatigue strength value associated with a specific life to be achieved ($2x10^6$ cycles for Eurocode Standard and IIW Recomendations), *ii)* declivity of log S-log N line and *iii)* points of transition between usual, high and presumed infinite fatigue life. Distinct materials or structural components usually present completely different S-N curves. However, Eurocode standard and IIW Recommendations consider that a family of S-N curves has a constant declivity and the same points of transition between ordinary, high and infinite life. So, the parameter that essentially represents the fatigue life performance is the fatigue strength value for a fixed number of cycles of load. Inside Eurocode standard, this parameter is called “Detail Category”, while the IIW Recommendations adopt the name “FAT Number”. The AWS code nominates the S-N curves by letters and all the S-N curves have the same declivity (exception to the “F” category), but different transition points of the finite and infinite life. This transition point corresponds to the strength reference value.

The three reference procedures – Eurocode, AWS and IIW – are limited to structural steels with ultimate strength lower than or equal to 690 MPa. However, all of these procedures ultimately include stainless steels in the family of structural materials. Nevertheless, no one of them supply specific S-N diagrams of any type of stainless steel. So, the designer has to consider two possibilities: *i)* assign for any stainless steel the same fatigue behavior of an ordinary structural steel or *ii)* proceed with a set of fatigue tests to validate the joint design process.

Present work shows S-N diagrams of butt welded joints of austenitic AISI 316 L stainless steel, loaded with repeated transversal load with a tension ratio of R = 0. The specimens were robot-welded in a GMAW process. Three cases were evaluated: *i)* not welded specimens, to serve as a reference curve, *ii)* welded specimens in a raw form and *iii)* welded specimens with face and root reinforcements removed by a grinding process.

The procedures adopted for specimens manufacturing and testing are explained in sequence.

2. EXPERIMENTAL DETAILS

2.1. CHARACTERISTICS OF THE MATERIAL AND GEOMETRY OF THE SPECIMENS

Specimens of the design shown in Fig. 1, based on ISO/TR 14345 (2012), were manufactured from the same plate of AISI 316 L austenitic stainless steel, with a thickness of 6 mm.

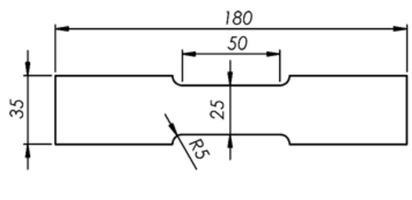

Figure 1 – Dimensions of the specimens.

The most relevant chemical elements of the material, obtained by optical spectrometry, are shown in Table 1.

Chemical Elements (% weight)								
C	Si	Mn	P	S	Cr	Ni	Mo	N
0,03	0,499	1,35	0,024	0,013	17,8	9,63	2,11	0,075

Table 1 – Chemical elements of the AISI 316L plate used to manufacture the specimens.

The mean yield and tensile strengths of the material were determined by tensile testing to be: *i)* in welded specimens: $S_y = 439\ MPa$ and $S_{ut} = 617\ MPa$ and *ii)* in no weld specimens (parent metal): $S_y = 411\ MPa$ and $S_{ut} = 601\ MPa$. A set of five specimens, all aligned with the rolling direction, were adopted in each case.

Figure 2 shows the tensile test curves corresponding to, respectively, parent metal and welded specimens.

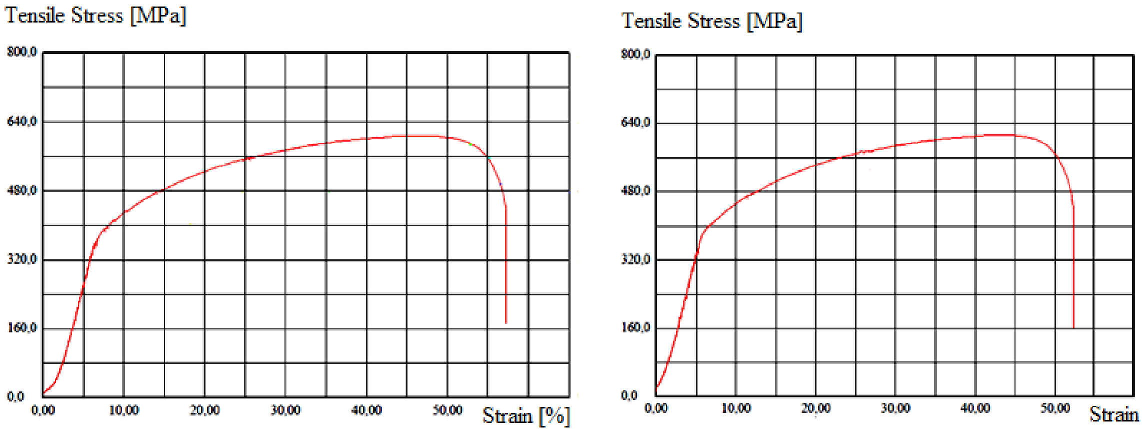

(a) (b)

Figure 2 – Tensile test curves of: a) no weld specimen and b) welded specimen.

The original material showed a predominantly austenitic microstructure with polygonal austenite grains and the presence of twinning planes, as shown in Figure 3.

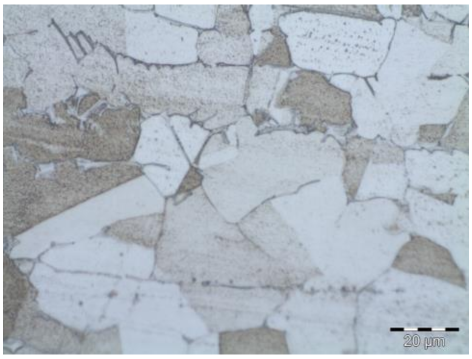

Figure 3 – Austenitic microstructure of parent metal.

2.2. WELDING OF TEST PLATES AND MACHINING OF THE SPECIMENS

According to AWS D1.1 (2010), there is no need of a special preparation in case of a butt joint when plate thickness is lower than 8 mm. A root opening of 1.2 mm was adopted. Both parts were constrained, during the welding process, by means of bolted frames.

The GMAW welding process was carried out by a robot. The welding source presents a characteristic of constant tension, with voltage regulation in ranges and the possibility of continuous adjusting of the wire feed speed. The electrode wire class adopted was the E316LSi AWS, with a diameter of 1.0 mm. The shielding gas was Ar + 2% O_2 with a flow rate of 16 l/min. Figure 4 shows a transversal cut macro view of a resultant beam.

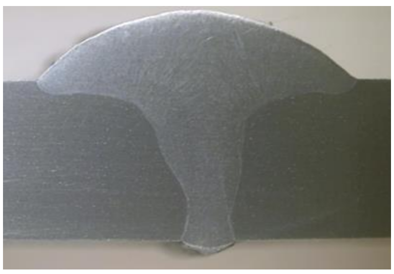

Figure 4 – Cross view of the resultant beam.

It is possible to observe the complete fusion and the good penetration provided by the welding process. The reinforcement geometry was suitable, with a height of approximately 2.7 mm in the face and 0.5 mm in the root, which is in accordance with AWS D1.6 (2007). No relevant porosities or inclusions were observed in the weld bead region.

Figure 5 shows a micro view of the region of transition between the weld fusion zone and parent metal, where it is observed the already expected grain growth at the heat affected zone.

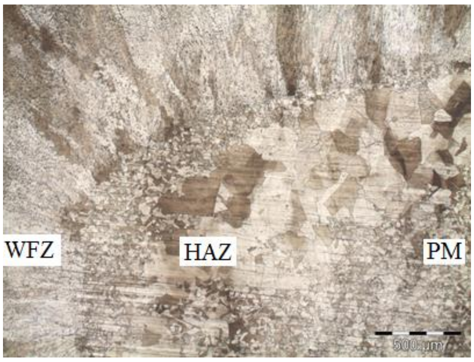

Figure 5 – Microstructure of the region of transition between Welded Fusion Zone and Parent Metal.

After the welding process, plates were plasma cut transversely to the bead, in order to obtain five stripes. These stripes were machined in a CNC milling machine to produce the neck profile to the specimens. Afterwards, the lateral faces of the machined region of the neck were manually sanded in a longitudinal direction.

As observed, the original test plates were dimensioned to obtain 5 specimens each. A total number of 6 test plates were manufactured, resulting in 15 specimens for “as welded” and 15 specimens for “welded and ground” tests. The selection of specimens for each group was arbitrary. Another 12 specimens, assigned to compose de S-N diagram of the original metal, were cut and machined to the same final geometry, but without passing by welding process.

The specimens assigned to have the bead reinforcements removed, passed by a posterior cylindrical grinding operation in a proper machine, in order to obtain the scratches aligned with the direction of load. The final surface finish achieved an approximate value of Ra = 3.2 μm. The grinding process was confined only to the bead region.

2.3. FATIGUE TESTS

Fatigue tests were performed in a servo hydraulic machine, at room temperature. The load frequency ranged from 15 to 20 Hz and the value of stress ratio was R = 0. The specimens were marked, so it would be possible to identify, if necessary, the locus over the total plate or inside the specific test plate from where the specimen was taken.

2.3.1. FATIGUE LIFE ESTIMATIVE BASED IN EUROCODE, IIW AND AWS

Some differences between Eurocode, IIW and AWS references should be initially explained. All these codes are based on the classification method, so the weld joints are ordinated in several categories, depending on the life achieved by the specimens in a specific set of direction and value of load.

As said before, both Eurocode standard and IIW recommendations adopt the normal or shear tension range corresponding to a fatigue life of 2 million cycles as the nominal parameter of an S-N diagram. On the other hand, AWS code adopts a nomenclature based in letters – A, B, B’, C, D, E and E’, so the nominal parameter is not so clear. However, the equations of this code adopt, as the reference point, the transition between finite and infinite life, which is different for each S-N curve.

A butt joint of a structural steel, with no significant misalignment, subjected to a tension transversal to bead line, is classified as showed in table 2.

		Eurocode	IIW	AWS
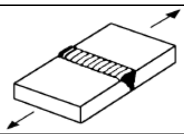	as welded	Detail Category 71	FAT Number 71	Category C
	welded and ground	Detail Category 112	FAT Number 125	Category B

Table 2 – Categories of a butt welded joint in accordance with Eurocode, IIW and AWS.

Figure 6 shows the corresponding S-N diagrams for the cases indicated in table 2.

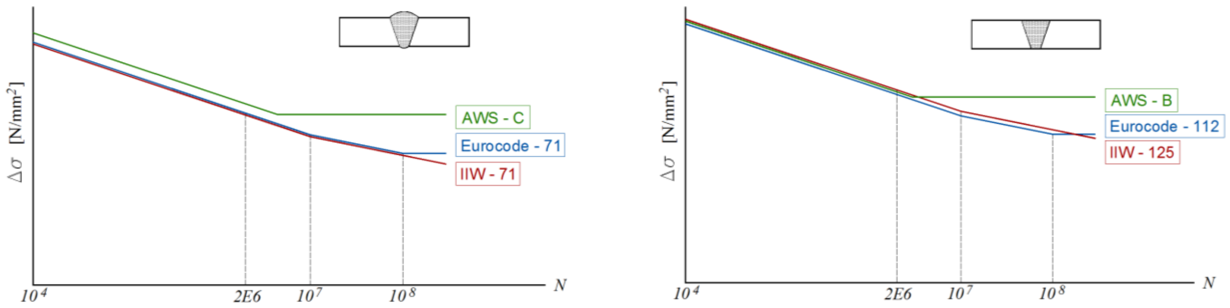

(a) (b)

Figure 6 – Categories of butt welded joints in accordance with Eurocode, IIW and AWS:
a) for the "as welded" case, and b) for "welded and ground" case.

Figure 7 shows the corresponding S-N diagrams of not welded ordinary steel plates used in structural applications.

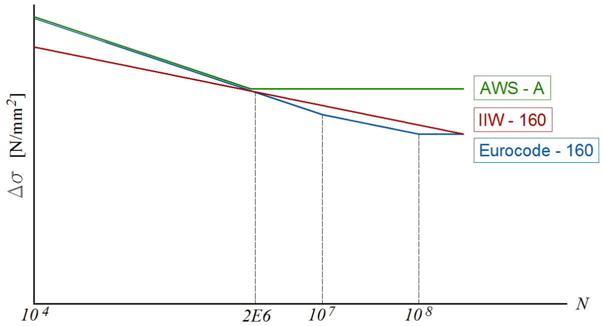

Figure 7 – Categories of the parent metal, in accordance with Eurocode, IIW and AWS.

In accordance with the three reference codes adopted, the S-N diagrams shown in Fig. 6 and Fig. 7 can be applied for stainless steel assessment. So, these diagrams were used to specify the different stress ranges values adopted in the tests. This assumption means a simplified approach, whereby a stainless steel (ferritic or austenitic in case of welded joints) has a similar fatigue behavior and fracture toughness of a structural steel (ferritic or bainitic).

2.3.2. EXPERIMENTAL RESULTS

A. FATIGUE DIAGRAM OF THE GROUP OF "AS WELDED" SPECIMENS

The order of specimens and load ranges was chosen in a completely randomly way. Ten specimens were specified to the tests, divided in five load ranges. The remaining five specimens were put apart, to be used in case of necessity of additional tests. The values of loads were selected adopting two references: *i)* the yield strength obtained in tensile test (the spread was arbitrated into *0.3* and *0.7Sy*) and *ii)* the Eurocode, IIW and AWS diagrams of fig. 6.

Figure 8 shows the resultant S-N diagram, corresponding to the data presented in Tab. 3.

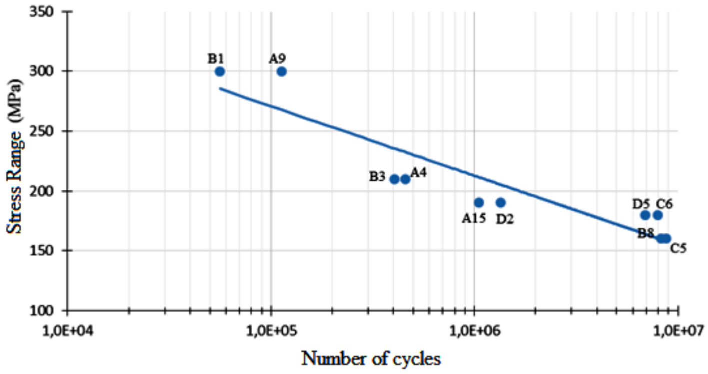

Figure 8 – S-N diagram corresponding to the "as welded" group of specimens.

Stress Range (MPa)	Specimen	Life (cycles)	Fracture site
160	B8	8.237.501	HAZ
	C5	8.791.977	HAZ
180	C6	7.955.213	HAZ
	D5	6.930.000	HAZ
190	A15	1.053.141	HAZ
	D2	1.351.089	HAZ
210	A4	455.274	HAZ
	B3	404.343	HAZ
300	A9	112.506	HAZ
	B1	56.174	HAZ

Table 3 – Results obtained for the “as welded” group of specimens.

All the specimens presented the final fracture at the toe region, corresponding to the heat affected zone. Figure 9 shows one of the specimens after fracture. The regions of crack initiation and final fracture are indicated. It is worth to observe the significant deformation at the final fracture region, which indicates that the welded material presented a good ductile behavior.

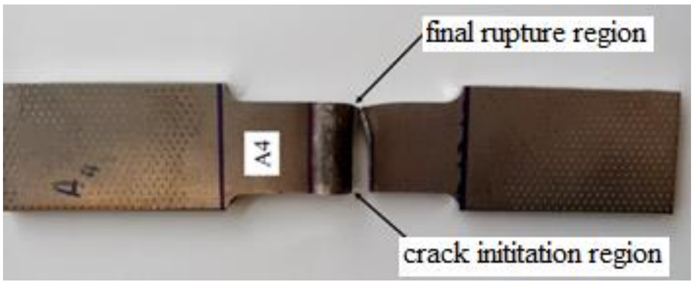

Figure 9 – Final aspect of specimen after fracture.

Figure 10 shows the same diagram of Fig. 8, indicated with AISI 316 L designation, plotted together with Eurocode, IIW and AWS curves of structural steels. The figure highlights two important discrepancies: *i)* the curve of stainless steel presents a lower declivity and *ii)* all the code curves apply, and have a quite strong degree of safety, for life expectative greater than 10^5 cycles. However, in case of life expectative values bellow 10^5 cycles, all the code diagrams provide an overestimated admissible stress range.

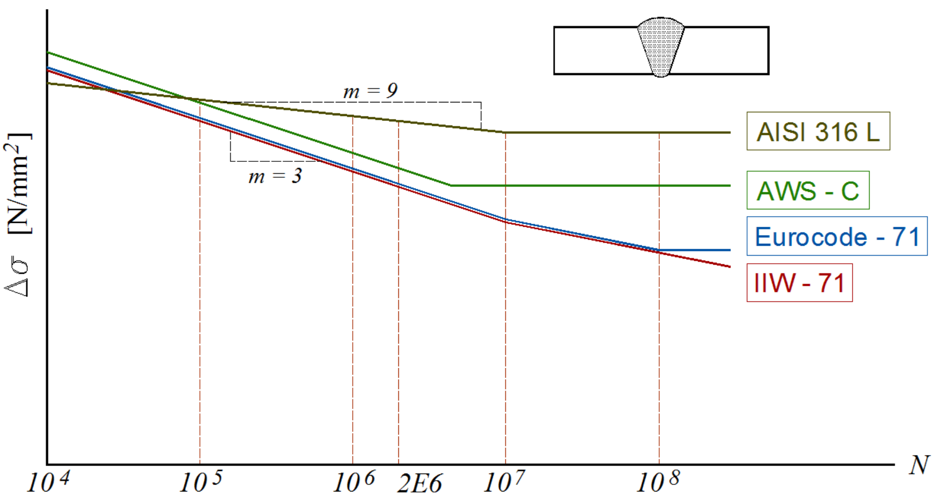

Figure 10 – S-N diagram for “as welded” group of specimens, in comparison with Eurocode, IIW and AWS data.

B. FATIGUE DIAGRAM OF THE GROUP OF "WELDED AND GROUND" SPECIMENS

The results of fatigue tests on specimens with machined and ground welded reinforcements, to each applied stress range, are shown in Tab. 4 and the corresponding S-N diagram is presented in Fig. 11.

Stress Range (MPa)	Specimen	Life (cycles)	Fracture location
250	B13	8.031.925	no fracture
300	C1	5.000.253	no fracture
	D10	3.000.241	no fracture
330	D9	530.508	HAZ
350	D12	69.315	WFZ
370	A12	215.057	HAZ
	B14	305.519	HAZ

Table 4 – Results of tests obtained in the "welded and ground" group of specimens.

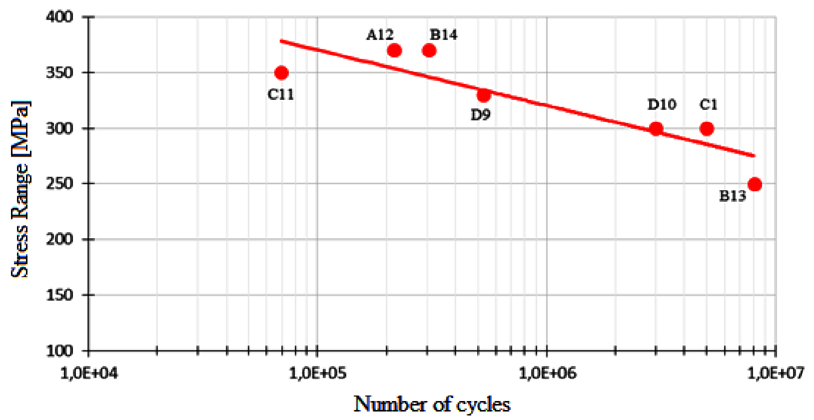

Figure 11 – S-N diagram corresponding to the "welded and ground" group of specimens.

Figure 12 shows the S-N diagram of Fig. 10, plotted together with Eurocode, IIW and AWS curves of structural steels. The same observations explained in the previous case of "as welded" specimens are valid, however, the S-N diagram of the "welded and ground" exhibit an even lower declivity.

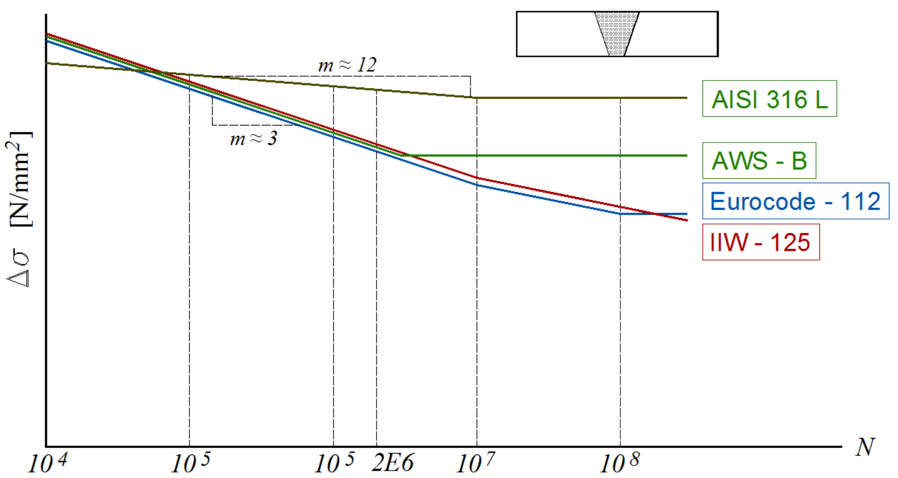

Figure 12 – S-N diagram for "welded and ground" group of specimens, in comparison with Eurocode, IIW and AWS data.

C. FATIGUE DIAGRAM OF THE PARENT METAL

The results of fatigue tests over the "no weld" group of specimens, to each applied stress range, are shown in Tab. 5 and the corresponding S-N diagram is presented in Fig. 13.

Stress Range (MPa)	Specimen	Fatigue life (cycles)	Status
210	E18	10.000.000	test stopped
250	E11	7.558.706	fractured
	E16	8.389.381	fractured
290	E1	613.455	fractured
	E9	985.997	fractured
300	E2	297.462	fractured
	E3	209.462	fractured
348	E17	183.095	fractured
	E15	308.449	fractured
385	E19	139.530	fractured
	E22	161.717	fractured

Table 5 – Results of tests obtained in the "no weld" group of specimens.

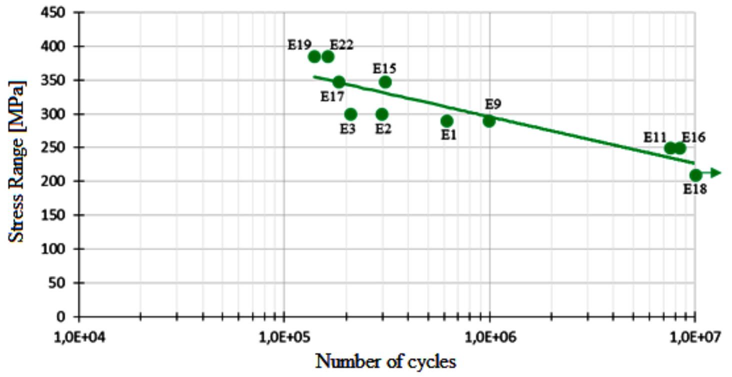

Figure 13 – S-N diagram corresponding to the "no weld" group of specimens.

Figure 14 shows the S-N diagram of Fig.13, plotted together with Eurocode, IIW and AWS curves of structural steels. It is observed again the low linear declivity on the log-log resultant curve.

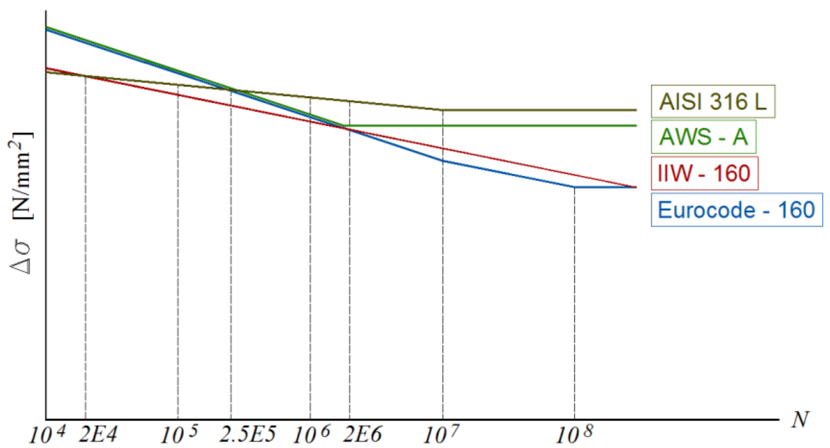

Figure 14 – S-N diagram obtained in the "no weld" group of specimens, in comparison ith Eurocode, IIW and AWS data.

Comparing this final diagram with AWS-A and Eurocode-160 reference curves, it is evident a division point at 2.5e5 cycles. For a lower stress range than the corresponding to this fatigue life, the AISI 316 L presents a better response. However, at high stress ranges, AISI 316 L presented a worst performance under dynamic loads. If the IIW-160 curve is adopted as the reference, the division point is at 2e4 cycles.

2.3.3. RESUME OF RESULTS AND DISCUSSION

Figure 15 puts together the S-N diagrams and summarizes the results obtained in the three test cases.

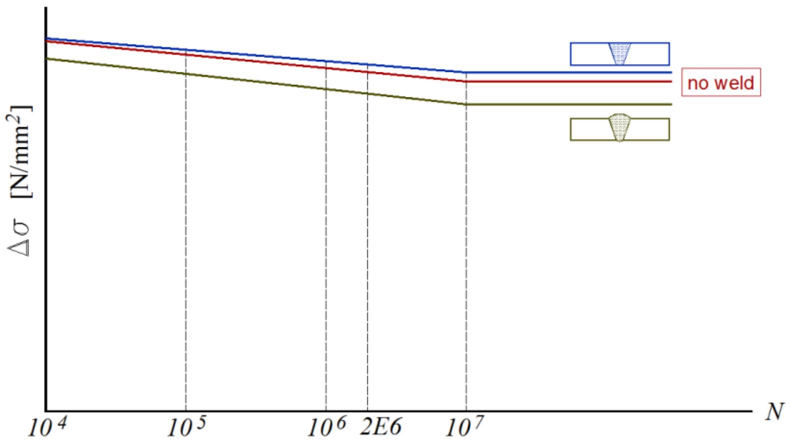

Figure 15 – S-N diagrams obtained in the three groups of specimens.

Examining all the diagrams obtained, it is observed that the fatigue behavior of the austenitic AISI 316 L specimens is quite different in relation to the ferritic or bainitic structural steels presented in Eurocode, IIW and AWS instructions. In spite of the relative low yield strength of the AISI 316 L, all the specimens presented an important plastic deformation before fracture, which is an indicative of significant fracture toughness. The first characteristic can be associated with the poor performance demonstrated at high stress range values, while the second one is associated with the small declivity of the S-N diagrams obtained. So all the tests performed indicate a superior performance under fatigue at medium and low stress range values. The division line between these two zones, of upper and lower fatigue performance, with some variation among the groups of specimens tested, is represented by a life of 10^5 cycles. So, the procedure of welded joints assessment suggested by the reference codes, in the case of a butt joint made of austenitic stainless steel, seems to be quite conservative for medium and low stress range values and, on the contrary, provides underestimated safety parameters in cases of high stress ranges.

Another result observed is the superior performance presented by the group of specimens in which the reinforcements were removed. In this case, the procedure prescribed by the reference codes is adopting S-N diagrams that, as shown in Fig. 6, are superior to those of a butt joint with original reinforcements, but are lower than the curves associated with plates, flats or extruded tubes.

On the other hand, Branco et al. (1999) sustains that a carefully performed reinforcement removal causes an approximation of the butt joint S-N diagram to the one expected for plates and flats, which is in accordance with the results obtained in present work. As observed in Fig. 15 the S-N diagram of the “welded and ground” specimens is slightly above the corresponding to the “no welded” group. This unexpected result may be explained by the lightly greater mechanical strength shown by the welded specimens in the performed tensile tests, as well as the natural data dispersion of fatigue tests.

3. CONCLUSIONS

This work presented the tests performed to trace S-N diagrams of butt welded joints, subjected to transversal loading, employing AISI 316 L stainless steel specimens, which were disposed in three different groups: a) specimens with normal weld beads - no machining of bead reinforcement, b) specimens with machined weld beads, in order to remove the face and root reinforcements and c) specimens for base metal evaluation (no weld).

It was observed a different behavior of the austenitic stainless steel when compared with the ferritic and bainitic structural steels covered by Eurocode, IIW and AWS codes. It was observed a worst fatigue performance of the AISI 316 L under high stress range values and, on the contrary, a significant better response from middle to low stress ranges. So, the assumption that an austenitic stainless steel could present the same fatigue behavior of an ordinary ferritic or bainitic structural steel could not be applied in case of a butt welded joint. More tests should be performed in order to collect robust data, covering important aspects correlated: influence of the R stress factor, welding in field conditions, evaluation of stress concentration in the specimens and others. However, all the results obtained point to the necessity of creating a special family of S-N diagrams, specifically addressed to austenitic steels.

Finally, it was observed a significant increase of fatigue performance by carefully removing the bead face and root reinforcements. This relatively simple post welding process was responsible for providing a performance similar to that expected for the parent metal.

The results obtained indicate that the austenitic stainless steel is suitable for structural applications, which is already observed in current civil and mechanical structures. Because of the characteristics of this material, it is expect a worldwide increment of use in structural components like girders, trusses, buildings and bridges.

4. ACKNOWLEDGEMENTS

The authors would like to acknowledge the major contribution from the colleagues of the Manufacturing Laboratories of FURG, in particular Dr. Douglas Bezerra de Araujo and engineer Daniel Souza.

The authors also would like to thank the aid from Manufacturing Laboratory of the Federal Institute IF-Sul, Pelotas, for proceeding with the CNC milling of the specimens. Our gratefulness extends also to SENAI, Rio Grande, which was responsible for the grinding process applied to the specimens.

Finally, the authors would like to thank FAPERGS for the Master Scholarship.

5. REFERENCES

American Standard AWS D1.1/D1.1M:2010 – *Structural Welding Code – Steel*.

Branco, C.M., Fernandes, A.A., Castro, P.M.S.T., 1999. *Fadiga de Estruturas Soldadas*. Fundação Calouste Gulbenkian, Lisboa, 2nd ed.

European Standard prEN 1993-1-9:2003 - *Eurocode 3: Design of Steel Structures - Part 1.9: Fatigue*.

Haldimann-Sturm, S.C., Nussbaumer, A., 2008. "Fatigue Design of Cast Steel Nodes in Tubular Bridge Structures". *International Journal of Fatigue,* Vol. 30, Issue 3, March 2008, Pages 528–537.

Hobbacher A., 2008. *Recommendations for Fatigue Design of Welded Joints and Components*. International Institute of Welding, doc. XIII-2151r4-07/XV-1254r4-07. Paris, France.

International Standard ISO/TR 14345:2012(E). *Fatigue – Fatigue Testing of Welded Components – Guidance.*

Lassen, T., Récho, N., 2006. *Fatigue Life Analyses of Welded Structures: Flaws*. ISTE, London, England.

Nussbaumer, A., Herion, S., Veselcic, M. and Dietrich, R., 2010. "New S-N curves for Details in Bridges with Steel Truss Tubular Superstructure". *Proceedings of the 13th International Symposium on Tubular Structures*, ISTS 13, Hong Kong.

Wardenier, J., Dutta, D., Yeomans, N., Packer, J.A. and Bucak, Ö., 1995. *Design Guide for Structural Hollow Sections in Mechanical Applications*, TÜV-Verlag, Köln, Germany.

Zhang, Y-H., Maddox, S.J., 2009. "Fatigue Life Prediction for Toe Ground Welded Joints". *International Journal of Fatigue*, V. 31, p. 1124–1136.

Zhao,X.L., Herion,S., Packer,J., Puthli,R., Sedlacek,G., Wardenier,J., Weynand,K., Van Wingerde,A. and Yeomans,N., 2001. *Design Guide for Circular and Rectangular Hollow Section Welded Joints under Fatigue Loading*, TÜV-Verlag, Köln, Germany.

6. RESPONSIBILITY NOTICE

The authors are the only responsible for the printed material included in this paper.